

Virtual Screening Discovery of New Acetylcholinesterase Inhibitors Issued from CERMN Chemical Library

Jana Sopkova-de Oliveira Santos,^{†,*} Aurelien Lesnard,[†] Jean-Hugues Agondanou,[†] Nathalie Dupont,^{†,‡} Anne-Marie Godard,[†] Silvia Stiebing,[†] Christophe Rochais,[†] Frederic Fabis,[†] Patrick Dallemagne,[†] Ronan Bureau,[†] and Sylvain Rault[†]

[†] Centre d'Etudes et de Recherche sur le Médicament de Normandie, UPRES EA-4258, FR CNRS INC3M, Université de Caen, UFR des Sciences Pharmaceutiques, bd Becquerel, 14032 Caen Cedex, France

Received December 18, 2009

In our quest to find new inhibitors able to inhibit acetylcholinesterase (AChE) and, at the same time, to protect neurons from beta amyloid toxicity, i.e., inhibitors interacting with the catalytic anionic subsite as well as with the peripheral anionic site of AChE, a virtual screening of the Centre d'Etudes et de Recherche sur le Médicament de Normandie (CERMN) chemical library was carried out. Two complementary approaches were applied, i.e., a ligand- and a structure-based screening. Each screening led to the selection of different compounds, but only two were present in both screening results. In vitro tests on AChE showed that one of those compounds presented a very good inhibition activity, of the same order as Donepezil. This result shows the real complementary of both methods for the discovery of new ligands.

INTRODUCTION

Alzheimer's disease (AD) is a neurological disorder characterized by a significant decrease in hippocampal and cortical levels of the neurotransmitter acetylcholine (AChE), leading to severe memory and learning deficits.¹ According to the cholinergic hypothesis,² inhibition of AChE in the central nervous system can alleviate these deficits. During the past decade, several cholinergic drugs have been launched on the market, including the synthetic compounds Tacrine,^{3,4} Donepezil (E2020),^{5–8} and Rivastigmine⁹ as well as the alkaloid (–)-galanthamine.¹⁰ These drugs are efficient for the treatment of mild to moderate AD. Among them Donepezil,^{5–8} a dimethoxyindanone derivative, represents a special class of AChE inhibitors named gorge-spanning inhibitors.

Crystal structures of AChE revealed that its active site, the catalytic triad Serine200–Histidine440–Glutamic acid327 (Ser200–His440–Glu327), which is responsible for hydrolyzing the ester bond of ACh, lies at the bottom of a deep and narrow gorge called either the active-site or the aromatic gorge. Nearly 70% of its surface is lined by rings of 14 conserved aromatic amino acids.^{11,12} Two aromatic side chains, tryptophan (Trp84) and phenylalanine (Phe330) lie in the proximity of the catalytic triad and constitute the binding site called the catalytic anionic subsite. Crystallographic studies of AChE revealed a second binding site within the active site, named the peripheral anionic site. It is situated at the mouth of the gorge and contains two aromatic side chains, tyrosine (Tyr70) and Trp279. Simultaneous binding to the catalytic anionic subsite and the peripheral anionic site is responsible for the enhanced

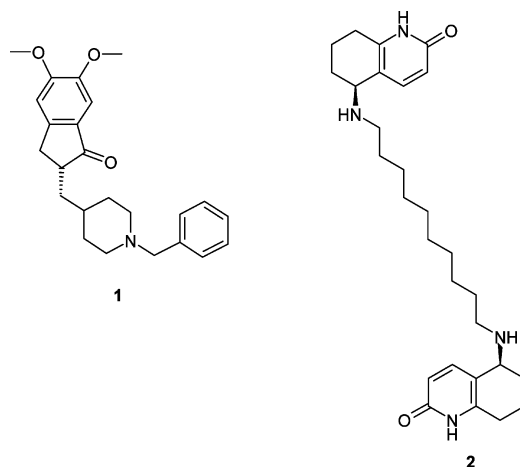


Figure 1. Diagram of two AChE inhibitors reported in the literature and used in this study.

binding of gorge-spanning ligands, such as Donepezil, decamethonium,¹³ BW284c51,¹⁴ and ambenonium.¹⁵ Recent biochemical studies have shown that the peripheral anionic site is also implicated in promoting aggregation of the beta-amyloid (A β) peptide responsible for the neurodegenerative process in AD.^{16–18} Thus, the design of inhibitors interacting with the peripheral anionic site is of clear potential interest for treatment of AD.¹⁹

We applied virtual screening of our own chemical library to obtain new inhibitors which will be able to inhibit AChE and, at the same time, to protect neurons from A β toxicity. This work was based on two AChE inhibitors belonging to the gorge-spanning family: Donepezil (IC₅₀ = 20 \pm 10 nM),²⁰ whose long and selective action and manageable adverse effects make it a lead compound in this pharmacological series (Figure 1, compound 1), and (S,S)-(–)-bis(10)-hupyrindone (IC₅₀ = 2.4 \pm 0.1 nM),²¹ a potent bivalent ligand (Figure 1, compound 2) designed to span both sites. Crystal

* Corresponding author. Telephone: (33)2-31-56-68-21. E-mail: jana.sopkova@unicaen.fr.

[‡] Current address: Unité CNRS FRE 3043–Laboratoire CSPBAT, Equipe C2B, UFR SMBH–Université Paris 13, 74 rue Marcel Cachin, 93017 Bobigny Cedex, France.

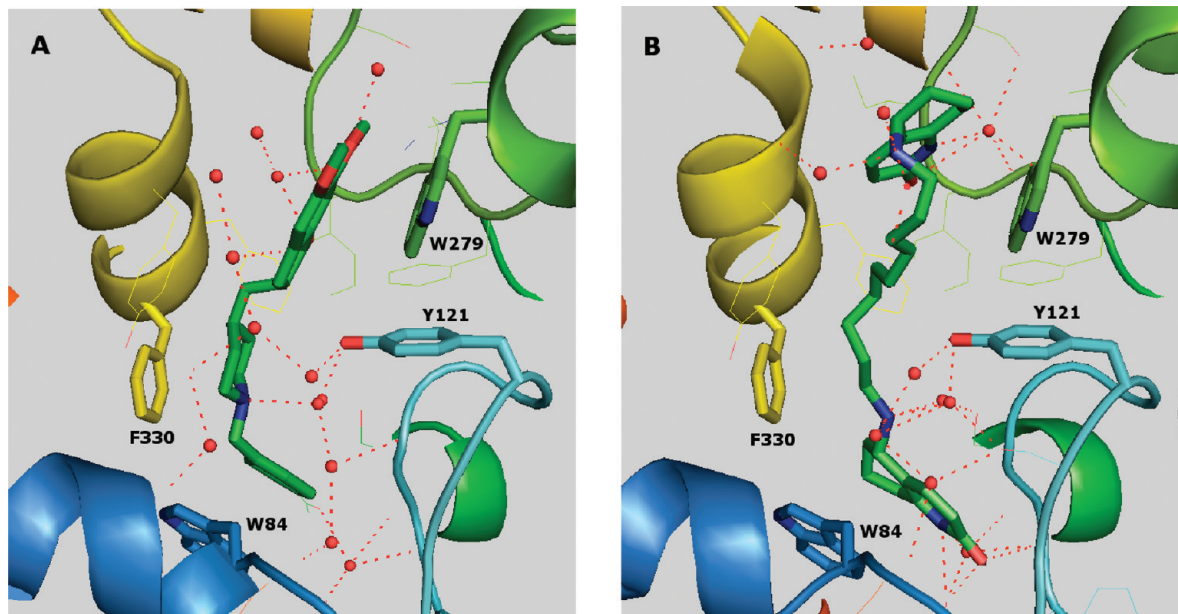


Figure 2. The AChE binding site from the X-ray structure of complexes with: (A) Donepezil (PDB ID: 1EVE) and (B) (*S,S*)-(-)-bis(10)-hupyridone (PDB ID: 1H22). The protein is represented as a ribbon, the side chains of binding site residues are in a stick representation, and the red balls represent water molecules. This figure was made with PYMOL (DeLano Scientific, LLC, San Francisco, CA, 2002).

structures of complexes, a fundamental point for the selection of these derivatives, are available for both ligands.

The crystal structure of *Torpedo californica* AChE cocrystallized with Donepezil⁶ showed it to lie along the axis of the active-site gorge, making interactions with the two highly conserved tryptophan residues, Trp84 of the catalytic anionic subsite and Trp279 of the peripheral anionic site, but with no interactions with the catalytic triad (Figure 2). Donepezil (1) binds by π -stacking interactions of the indanone ring with Trp279 and of the benzyl ring with Trp 84. A π -cation interaction occurs between the charged nitrogen of the piperidine ring and the phenyl ring of Phe330.²² The interaction of Donepezil in the active site is completed via a cluster of hydrogen bonds (H-bonds) through water molecules present in the active site. For example, the charged nitrogen of the piperidine ring is related by H-bonds across several water molecules to Tyr121. The crystal structure of *Torpedo californica* AChE cocrystallized with (*S,S*)-(-)-bis(10)-hupyridone (2)²³ showed that one of the aminoquinolone fragments interacts by π -stacking with Trp 84 and that the amide group of aliphatic chain is situated in the proximity of the Phe330 aromatic ring. In this crystal structure, the amide group is also linked via H-bonds with waters to Tyr 121. The other aminoquinolone fragment occupies the peripheral anionic site, but it is somewhat distant from Trp279 compared to that of the Donepezil indanone ring position.

Since we were looking for new ligands capable of interacting with both the 'catalytic' and 'peripheral' anionic sites, we carried out two virtual screens of our chemolibrary, starting from crystallographic data for the two complexes. In the first approach, a three-dimensional (3D) pharmacophore was defined on the basis of active 3D conformations of the two gorge-spanning AChE inhibitors, while the second screening was based on the active-site topology.

MATERIALS AND METHODS

The chemical library (CERMN database, <http://www.cermn.unicaen.fr/>) contained at the screening date 6626 compounds resulting from different research programs carried out in our laboratory in the field of medicinal chemistry.

Virtual Screening by Docking. The Protein Data Bank (PDB) contains several AChE complexes with small molecules bound to the active site. The major difference in the active-site conformation between these complexes is the orientation of Phe330. This side chain controls access to the bottom of the gorge and can adopt three major conformations, an open, a closed, and an intermediate access position. For gorge-spanning ligands, such as Donepezil or (*S,S*)-(-)-bis(10)-hupyridone, Phe330 adopts an open access position, while the overall protein structure, active site included, is very similar. The root-mean-square (rms) difference between AChE in these two complexes is about 0.2 Å (on all C α atoms). Since the two structures are similar, we chose the crystal structure of *Torpedo californica* AChE from the Donepezil complex (PDB ID: 1EVE⁶) for the virtual screening by docking. All water molecules were deleted before screening. We used standard tools of the ChemAxon Package (JChem 5.0.0, ChemAxon, <http://www.chemaxon.com>, 2008) to generate a 3D structure for each putative ligand in the CERMN chemolibrary.

The Gold program^{24,25} was employed to generate a set of docked conformations for each putative ligand. This program uses a genetic algorithm to explore conformational spaces and ligand binding modes. The genetic operators were 100 for the population size, 1.1 for the selection pressure (representing the relative probability that the best individual will be chosen as a parent), 5 for the number of subpopulations (island model), 100 000 for the maximum number of genetic applications, and 2 for the size of the niche used to increase population diversity. The weights were chosen so that crossovers and mutations were applied with equal

probability (95/95 for the values), and migration was applied 5% of the time. The calculation of the fitness functions is described in GoldScore and ChemScore.^{24,25} Generally, the higher the value calculated by the fitness function (in percentage), the higher the predicted affinity should be.

Pharmacophore-Based Virtual Screening. For the definition of the pharmacophore, the experimental 3D conformations of Donepezil⁶ and (*S,S*)-(-)-bis(10)-hupyrindone²³ (Figure 2) were selected from crystallographic data on the complexes (Donepezil from 1EVE⁶ and (*S,S*)-(-)-bis(10)-hupyrindone from 1H22²³). The definition of the pharmacophore was based on a common features alignment approach in Catalyst.²⁶ In this algorithm, the program identifies 3D spatial arrangements of chemical features that are common to the two molecules. The model consists of a 3D configuration of chemical functions surrounded by tolerance spheres. Principal and MaxOmitFeat values were set to 2 and 0, respectively, to ensure that all of their chemical features will be considered during the definition of the pharmacophore. Misses, feature misses, and complete misses were kept to default values: 1, 1, and 0, respectively. Superposition error, check superposition, and tolerance factor and the weights assigned to each chemical function were set to 1. The minimum interfeature distance was 3 Å. The initial features, for the definition of pharmacophores, were selected as a function of the structural characteristics of the ligands and the analysis of their interactions inside the receptor. They corresponded to hydrophobic aromatic, ring aromatic, and positive ionizable groups. For the CERMN chemolibrary, a quasi-exhaustive conformational search was done to generate, for each compound, a set of conformations (fast method of the Catalyst software). The energy range for the conformers, starting from the most stable conformation, was 20 kcal/mol with 250 conformations maximum by compound.

Using the pharmacophore generated as 3D queries, the CERMN database was searched for molecules fitting the pharmacophoric points.

In vitro Tests of AChE Biological Activity. Inhibitory capacities of selected compounds on AChE biological activity were evaluated using the spectrometric method of Ellman et al.²⁷ Lyophilized electric eel AChE (Type III, electric eel, Sigma) was dissolved in 0.2 M phosphate buffer, pH 7.4, to obtain an enzyme stock solution with 2.5 units·mL⁻¹ AChE activity. Acetylthiocholine iodide (Sigma) was used as a substrate of the enzymatic reaction, and 5,5-dithiobis-(2-nitrobenzoic) acid (DTNB, Sigma) was used as a label for cholinesterase activity. In the procedure, 1880 µL of 60 mg/500 mL DTNB dissolved in phosphate buffer, pH 7.4, were mixed with 40 µL each of test compound and enzyme stock solutions. After 5 min of pre-incubation, 40 µL of 10 mM acetylthiocholine iodide solution was added to the assay solution. The change in absorbance at 412 nm was recorded (AGILENT 8453 UV-vis spectroscopy system) during 10 min. A first screening of AChE activity was carried out at a 1×10^{-5} M concentration of the compounds under study. For the compounds with significant inhibition (>80%) after 4 min of reaction, the IC₅₀ values were determined graphically from log concentration-inhibition curves, using a range of 1×10^{-10} – 10^{-3} M concentrations of the test compounds.

We used a *Torpedo californica* and an electric eel AChE for the virtual screening and the in vitro test, respectively.

However, sequence analysis showed that there is only one residue difference in the active site, Phe330 in *Torpedo californica* is replaced by Tyr330 in electric eel (Figure 3), so we can consider the active sites as very similar.

RESULTS AND DISCUSSION

We used two kinds of virtual screening of the CERMN chemolibrary in the search for new and original gorge-spanning inhibitors of AChE, capable of interacting with both the catalytic and the peripheral anionic sites: first, a structure-based screening using a docking approach and, second, a ligand-based screening using a 3D pharmacophore.

The program Gold^{24,25} was used for the docking screen of the CERMN chemolibrary database with the crystal structure of AChE as a template, applying the GoldScore scoring function. One hundred compounds were, thus, selected, representing the best GoldScore values between 57 to 69%. Of these selected compounds, 81 molecules were evaluated by in vitro biological tests. Twenty-four compounds had an inhibition activity higher than 50% at 1×10^{-5} M ligand concentration, and among them, 4 compounds had a percentage of inhibition higher than 80% at this concentration (see compounds 3–6 in Table 2). The IC₅₀ of the four best compounds varied from (45 ± 10) to (540 ± 90) nM.

The second virtual screening was based on a 3D pharmacophore built from two AChE inhibitors: Donepezil and (*S,S*)-(-)-bis(10)-hupyrindone. Pharmacophore models are used to rationalize ligand–target interaction. Chemical function pharmacophore models consist of a number of ‘features’ that are located relative to each other in coordinate space, as points surrounded by a sphere of tolerance. Each sphere represents the region in space that should be occupied by a certain chemical function able of the kind of interaction specified by the feature type. Overall Catalyst²⁶ generated seven pharmacophores, which were divided into three groups by cluster analysis (average linkage) of the generated pharmacophores. The first cluster corresponding to two pharmacophores with the best scores exhibited three features: two aromatic rings and one positive ionizable. The second cluster corresponded to one aromatic, one hydrophobic, and one positive ionizable group (cluster of three pharmacophores). The last pharmacophore exhibited only two aromatic features. We selected the first pharmacophore model (Figure 4, Table 1), corresponding to two aromatic rings and one positive ionizable group. The aromatic features lie on the aromatic rings of the ligands, while the positively ionizable (basic) feature corresponds to the nitrogen of the piperidine ring in Donepezil and to the nitrogen on the aliphatic chain in (*S,S*)-(-)-bis(10)-hupyrindone (Figure 5). As described previously, the two aromatic ring features potentially interact with Trp 84 of the catalytic anionic subsite and with Trp 279 of the peripheral anionic site.

(*S,S*)-(-)-bis(10)-hupyrindone fits the pharmacophore perfectly (fit value of 3). For Donepezil, with 2.22, the fit value is slightly lower. In the virtual screening, the 40 compounds fitting all the characteristics of the pharmacophore and possessing a fit value superior to 2 were selected. Biological tests were carried out on 29 of these 40 compounds, with 16 derivatives showing an inhibition activity higher than 50% at a 1×10^{-5} M ligand concentration, and among them, ten

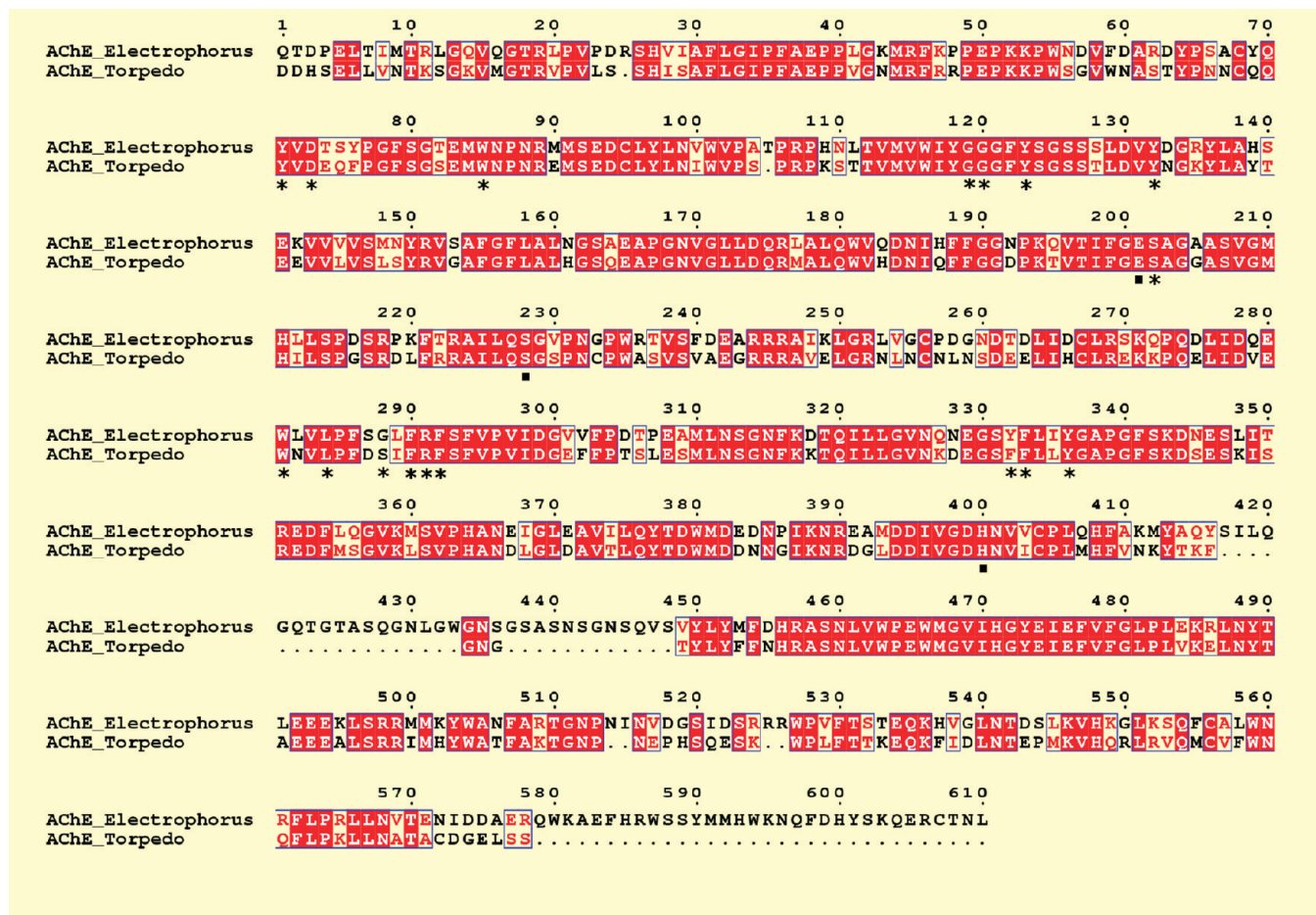


Figure 3. Amino acid sequence alignments of *Torpedo californica* and electric eel AChE. The residues shown in a red box indicated the identical residues, the asterisk (*) denotes residues of the AChE binding site and (■) denotes residues of the AChE catalytic triad. This figure was made with ESPript.

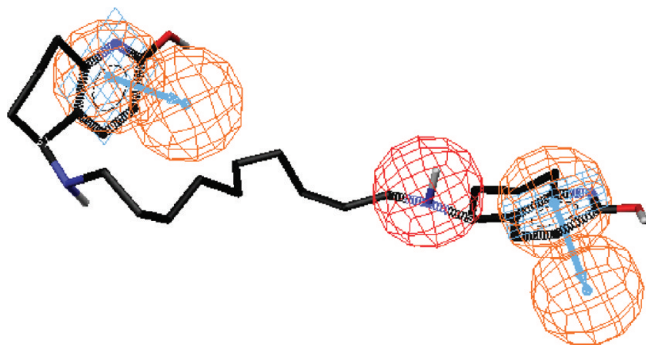


Figure 4. Pharmacophore aligned with (S,S)-(-)-bis(10)-hupyrindone from the X-ray structure of AChE/(S,S)-(-)-bis(10)-hupyrindone (1H22).

had an activity higher than 80% at this concentration. The IC_{50} of the best 10 compounds (3, 5, 7–14) varied from (45 ± 10) to (1370 ± 360) nM (see Table 2).

We note that the efficiency of this second screening is better than the structure-based screening (34% for the success rate). This result is interesting, though not so surprising. Indeed, the 3D pharmacophore was built on the basis of the known active conformation of two AChE inhibitors, so the conformation of ligands is exactly determined, and the nature and position of the chemical groups responsible for the interaction with AChE are fixed without any doubt. Another point concerns the basic group, which is responsible of π -cation interaction with Phe130, on the one hand, and

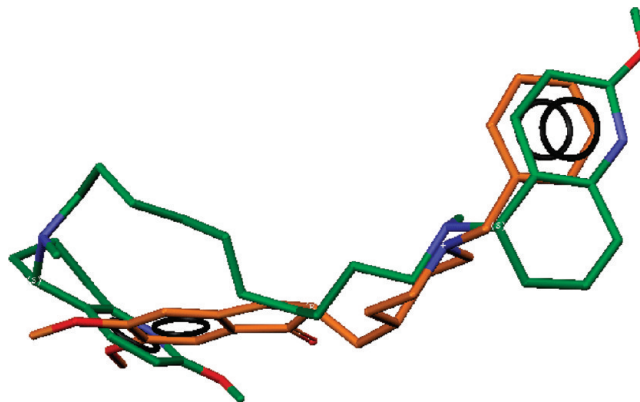


Figure 5. Superimposition between Donepezil (orange) and (S,S)-(-)-bis(10)-hupyrindone (green) by considering the pharmacophore.

interacts through H-bonds via water molecules with Tyr121 as well. Therefore, the removal of water molecules in the docking process decreases the importance of the basic group for binding, which is not the case in the pharmacophore approach.

Other 3D pharmacophores for AChE inhibitors have been published previously, for example, by Rollinger et al.²⁸ Their pharmacophore was built using galanthamine¹⁰ and was applied with success to screen a library of natural products. Their 3D pharmacophore is, however, different from ours because galanthamine represents another group of AChE

Table 1. Matrix Distances (in Å) for Selected Pharmacophore

| | Basic Center (P) | Aromatic ring 1 (IP1) | Aromatic ring 1 (PP1) | Aromatic ring 2 (IP2) | Aromatic ring 2 (PP2) |
|-----|---------------------|--------------------------|--------------------------|--------------------------|--------------------------|
| P | | | | | |
| IP1 | 9.3 | | | | |
| PP1 | 8.4 | 3 | | | |
| IP2 | 3.7 | 13.6 | 13.6 | | |
| PP2 | 4.7 | 15.4 | 13.2 | 3 | |

inhibitors. In the active-site gorge, it interacts with the acyl-binding pocket and the principal quaternary ammonium-binding site and but without any interaction with the peripheral anionic site.²⁹

The overlap of the resulting compounds of both our screenings showed that there are two molecules in common in the two sets: 3 and 5. In vitro tests showed that 3 is the compound with the best inhibition activity measured of all tested compounds with an IC_{50} of 45 ± 10 nM ($n = 6$). This derivative has also one of the best fit values with the pharmacophore (a value of 2.98 when two pharmacophore aromatic features were aligned by the two phenyl groups, and a value of 2.68 when they were aligned by the thienyl and the phenyl groups). It has also a relatively high value of GoldScore in the docking screening, about 61%, and was classed as the 27th best compound. The second compound, 5, with an IC_{50} of 514 ± 149 nM ($n = 3$) is the third best of the docking screening and fifth best of the pharmacophore screening in the in vitro tests. It also exhibited a good fit with the pharmacophore (a value of 2.80 when two pharmacophore aromatic features were aligned by the phenyl group and the pyrrole ring, and a value of 2.42 when they were aligned by the thienyl and the phenyl groups). In the docking screening, it has a relatively low GoldScore of about 58%, and it was classed as 86th.

The analysis of docking results showed that both compounds lie across the active-site gorge making interactions with the catalytic anionic subsite as well as with the peripheral anionic site (Supporting Information, Figure 1). Compounds 3 and 5 take positions very close to Donepezil in the crystal structure. The principal interaction of Donepezil seems to be reproduced, i.e., in both compounds, the piperazine ring is in good position for π -cation interaction and the π -stacking interactions with Trp279 of the peripheral anionic site and with Trp84 of the catalytic anionic subsite are also preserved. The stacking interaction with Trp 84 occurs through the benzene ring on piperazine ring in both compounds. The π -stacking interaction with Trp279 involves the thienimidazolidinone ring in compound 3 and the thienopyrrolopyrazinone ring in compound 5. The docking results showed that the phenyl group on thienimidazolidinone of compound 3 is oriented toward the entrance of the active-site gorge exposed to the solvent. Thus, a derivative with a smaller, or any hydrophobic group, at this position could enhance the affinity for AChE.

The superimposition between the docked conformations of these two compounds with our 3D pharmacophore model showed that the docking conformation of 3 aligns well with all three pharmacophore features (fit value of 2.24, Figure 6A), while the docking conformation of 5 also aligns by all three features, but the fit value of about 1.95 is lower (Figure 6B).

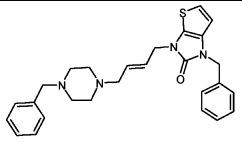
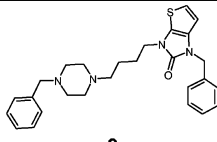
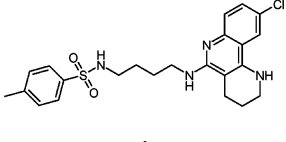
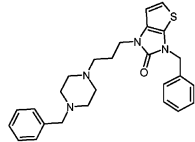
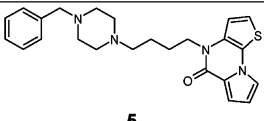
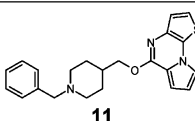
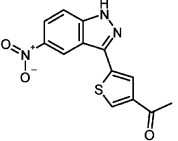
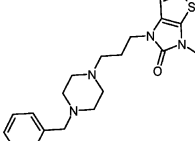
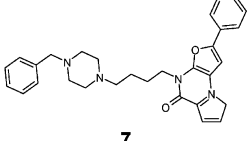
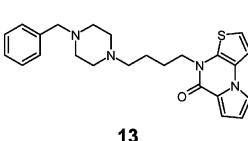
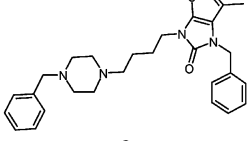
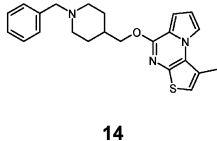
In vitro test showed that compound 4, selected only in the docking screening, exhibited an interesting IC_{50} of 93 ± 20 nM ($n = 6$). The docking pose showed that it binds principally by two π -stacking interactions involving the tetrahydrobenzopyridine moiety with Trp279 and the tolyl group with Trp84 (Supporting Information, Figure 1C). The π -cation interaction is absent for this compound, but two new direct H-bond interactions between 4 and residues of the enzyme are observed. The first is between the oxygen of the sulfonamide group and the hydroxyl group of Ser122 (distance O—O about 2.90 Å), and the second is between the amide group of the aliphatic chain and the hydroxyl group of Tyr121 (distance N—O about 2.70 Å). Thus, the absence of a π -cation interaction (absence of a basic group) for this compound seems to be compensated by the presence of two direct H-bonds.

A comparison of our new compounds with published AChE inhibitors (for this comparison we used AChE inhibitors that have been in the preclinical development state) shows that the compounds selected by pharmacophore virtual screening have some structural similarities with some of these compounds (Supporting Information, Figure 2 compounds 15 to 19).^{30–34} In the published compounds, we observed a similar sequence as in our compounds: a benzyl group attached to the piperidine, with this group then separated by a chain from the second aromatic ring. In our compounds discovered by pharmacophore screening, a benzyl group is always present and is attached to the piperidine or piperazine, while a second aromatic ring is attached at the other end of the compounds. The molecular diversity is greater for the compounds discovered by docking screening. The compound 19 (Supporting Information, Figure 2) is very interesting with respect to compound 4, since it also contains a sulfone group in proximity of the benzene ring.

CONCLUSION

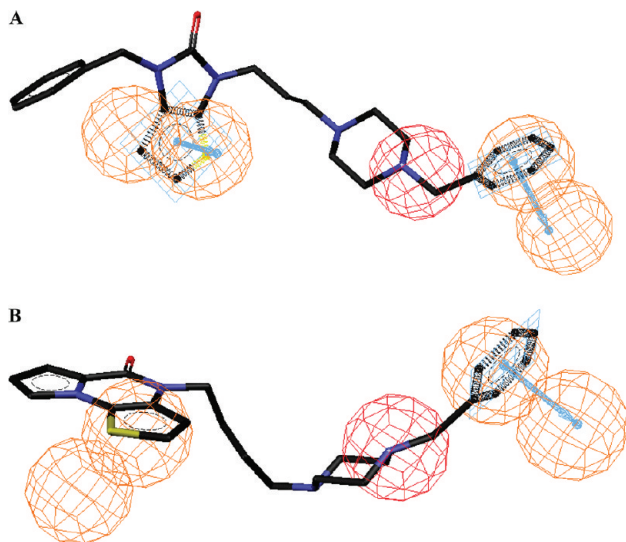
The two virtual screenings have identified 12 new chemically original compounds inhibiting AChE with an inhibition activity of the micromole order or better, including one of with an IC_{50} value close to that of Donepezil. The efficiency of 3D pharmacophore screening based on the exact conformation of ligands in the active site was very high (34%) with respect to classical structure-based drug design (docking approach), whose efficiency was about 5%. The analysis of compounds selected in pharmacophore screening showed that the basic feature as well as the two hydrophobic features were observed whatever the ligands. Thus, the information concerning the position of these two hydrophobic features, with respect to the basic group, is crucial to generate a good affinity for the receptor. The conformational search for each ligand in the pharmacophore approach is a quasi-exhaustive search. The pharmacophore method, thus, leads to a correct estimation of the ability of the ligand to interact with the hydrophobic area, corresponding to the catalytic anionic subsite and the peripheral anionic subsite of the AChE. The docking approach leads, however, to interesting complementary information concerning the possible orientations of the ligands in the AChE binding pocket. If we consider the alignment between the selected derivatives, we can see some new structural features. The docking results (Supporting Information, Figure 1C) showed that compound 4 does not

Table 2. Best Compounds from the Docking and Pharmacophore Virtual Screenings

| | IC ₅₀ (nM) | | IC ₅₀ (nM) |
|---|-----------------------|---|-----------------------|
|  3 | 45±10 |  9 | 298±159 |
|  4 | 93±20 |  10 | 1374±360 |
|  5 | 514±149 |  11 | 423±106 |
|  6 | 540±190 |  12 | 390±90 |
|  7 | 183±38 |  13 | 1283±55 |
|  8 | 553±109 |  14 | 527±246 |

interact through a π -cation interaction with Phe330. In this compound, the benzyl group is replaced by a benzene-sulfonamide group, which leads to interesting binding interactions in this region. Therefore, a sulfonamide group with the capacity to form direct H-bonds with the enzyme,

compared to that of a basic group, is an interesting alternative for pharmacomodulation in this area. As far as the π -stacking interactions with Trp27 of the peripheral anionic site is concerned, we see the same type of interaction through thienothiazolidine and benzonaphthylidene moieties of our compounds, thus, for this π -stacking interaction they could be considered as bioisosters.

**Figure 6.** Alignment between the conformation of 3 (A) and of 5 (B) from docking and the 3D pharmacophore.

ACKNOWLEDGMENT

We thank the CRIHAN (Centre de Ressources Informatiques de Haute Normandie) and the European Community (FEDER) for the molecular modelling software.

Supporting Information Available: Selected inhibitors positioned in the AChE binding site from docking studies, and diagram of selected AChE inhibitors in a preclinical state, reported in the literature. This material is available free of charge via the Internet at <http://pubs.acs.org>.

REFERENCES AND NOTES

- (1) DeKosky, S. T.; Scheff, S. W. Synapse loss in frontal cortex biopsies in Alzheimer's disease: correlation with cognitive severity. *Ann. Neurol.* **1990**, *27*, 457–464.
- (2) Bartus, R. T.; Dean, R. L. R.; Beer, B.; Lippa, A. S. The cholinergic hypothesis of geriatric memory dysfunction. *Science* **1982**, *217*, 408–414.

- (3) Davis, K. L.; Powchik, P. Tacrine. *Lancet* **1995**, *345*, 625–630.
- (4) Watkins, P. B.; Zimmerman, H. J.; Knapp, M. J.; Gracon, S. I.; Lewis, K. W. Hepatotoxic effects of tacrine administration in patients with Alzheimer's disease. *JAMA, J. Am. Med. Assoc.* **1994**, *271*, 992–998.
- (5) Kawakami, Y.; Inoue, A.; Kawai, T.; Wakita, M.; Sugimoto, H.; Hopfinger, A. J. The rationale for E2020 as a potent acetylcholinesterase inhibitor. *Bioorg. Med. Chem. Lett.* **1996**, *4*, 1429–1446.
- (6) Kryger, G.; Silman, I.; Sussman, J. L. Structure of acetylcholinesterase complexed with E2020 (Aricept): implications for the design of new anti-Alzheimer drugs. *Structure* **1999**, *7*, 297–307.
- (7) Nightingale, S. L. From the food and drug administration. *JAMA, J. Am. Med. Assoc.* **1997**, *277*, 10.
- (8) E-2020. Agent for Cognition Disorders Acetylcholinesterase Inhibitor. *Drugs Future* **1991**, *16*, 16–18.
- (9) Bar-On, P.; Millard, C. B.; Harel, M.; Dvir, H.; Enz, A.; Sussman, J. L.; Silman, I. Kinetic and structural studies on the interaction of cholinesterases with the anti-Alzheimer drug rivastigmine. *Biochemistry* **2002**, *41*, 3555–3564.
- (10) Greenblatt, H. M.; Kryger, G.; Lewis, T.; Silman, I.; Sussman, J. L. Structure of acetylcholinesterase complexed with (-)-galanthamine at 2.3 Å resolution. *FEBS Lett.* **1999**, *463*, 321–326.
- (11) Sussman, J. L.; Harel, M.; Frolow, F.; Oefner, C.; Goldman, A.; Toker, L.; Silman, I. Atomic structure of acetylcholinesterase from *Torpedo californica*: a prototypic acetylcholine-binding protein. *Science* **1991**, *253*, 872–879.
- (12) Axelsen, P. H.; Harel, M.; Silman, I.; Sussman, J. L. Structure and dynamics of the active site gorge of acetylcholinesterase: Synergistic use of molecular dynamics simulation and X-ray crystallography. *Protein Sci.* **1994**, *3*, 188–197.
- (13) Bergmann, F.; Wilson, I. B.; Nachmansohn, D. The inhibitory effect of stilbamidine, curare and related compounds and its relationship to the active groups of acetylcholinesterase. Action of stilbamidine upon nerve impulse conduction. *Biochim. Biophys. Acta* **1950**, *6*, 217–224.
- (14) Austin, L.; Berry, W. K. Two selective inhibitors of cholinesterase. *Biochem. J.* **1953**, *54*, 695–700.
- (15) Lands, A. M.; Hoppe, J. O.; Arnold, A.; Kirchner, F. K. An investigation of the structure-activity correlations within a series of ambenonium analogs. *J. Pharmacol. Exp. Ther.* **1958**, *123*, 121–127.
- (16) Alvarez, A.; Alarcon, R.; Opazo, C.; Campos, E. O.; Munoz, F. J.; Calderon, F. H.; Dajas, F.; Gentry, M. K.; Doctor, P. B.; De Mello, F. G.; Inestrosa, N. C. Stable complexes involving acetylcholinesterase and amyloid- β peptide change the biochemical properties of the enzyme and increase the neurotoxicity of Alzheimer's fibrils. *J. Neurosci.* **1998**, *18*, 3213–3223.
- (17) Alvarez, A.; Opazo, C.; Alarcon, R.; Garrido, J.; Inestrosa, N. C. Acetylcholinesterase promotes the aggregation of amyloid- β -peptide fragments by forming a complex with the growing fibrils. *J. Mol. Biol.* **1997**, *272*, 348–361.
- (18) De Ferrari, G. V.; Canales, M. A.; Shin, I.; Weiner, L. M.; Silman, I.; Inestrosa, N. C. A structural motif of acetylcholinesterase that promotes amyloid β -peptide formation. *Biochemistry* **2001**, *40*, 10447–10457.
- (19) Andreani, A.; Cavalli, A.; Granaiola, M.; Guardigli, M.; Leoni, A.; Locatelli, A.; Morigi, R.; Rambaldi, M.; Recanatini, M.; Roda, A. Synthesis and Screening for Antiacetylcholinesterase Activity of (1-Benzyl-4-oxopiperidin-3-ylidene)methylindoles and -pyrroles Related to Donepezil. *J. Med. Chem.* **2001**, *44*, 4011–4014.
- (20) Omran, Z.; Cailly, T.; Lescot, E.; Sopkova-de Oliveira Santos, J.; Agondanou, J.-H.; Lisowski, V.; Fabis, F.; Anne-Marie, G.; Stiebing, S.; Le Flem, G.; Boulouard, M.; Dauphin, F.; Dallemagne, P.; Rault, S. Synthesis and biological evaluation as AChE inhibitors of new indanones and thiaindanones related to donepezil. *Eur. J. Med. Chem.* **2005**, *40*, 1222–1245.
- (21) Wong, D. M.; Greenblatt, H. M.; Dvir, H.; Carlier, P. R.; Han, Y.-F.; Pang, Y.-P.; Silman, I.; Sussman, J. L. Acetylcholinesterase complexed with bivalent ligands related to Huperzine A: Experimental evidence for species-dependent protein-ligand complementarity. *J. Am. Chem. Soc.* **2003**, *125*, 363–373.
- (22) Meyer, E. A.; Castellano, R. K.; Diederich, F. Interactions with aromatic rings in chemical and biological recognition. *Angew. Chem., Int. Ed. Engl.* **2003**, *42*, 1210–1250.
- (23) Haviv, H.; Wong, D. M.; Greenblatt, H. M.; Carlier, P. R.; Pang, Y.-P.; Silman, I.; Sussman, J. L. Crystal packing mediates enantioselective ligand recognition at the peripheral site of acetylcholinesterase. *J. Am. Chem. Soc.* **2005**, *127*, 11029–11036.
- (24) Jones, G.; Willett, P.; Glen, R. C. Molecular recognition of receptor sites using a genetic algorithm with a description of desolvation. *J. Mol. Biol.* **1995**, *245*, 43–53.
- (25) Jones, G.; Willett, P.; Glen, R. C.; Leach, A. R.; Taylor, R. Development and validation of a genetic algorithm for flexible docking. *J. Mol. Biol.* **1997**, *267*, 727–748.
- (26) Catalyst, Accelrys Inc: San Diego, CA, 2003.
- (27) Ellman, G. L.; Courtney, K. D.; Andres, V.; Featherstone, J.; Featherstone, R. M. A new and rapid colorimetric determination of acetylcholinesterase activity. *Biochem. Pharmacol.* **1961**, *7*, 88–95.
- (28) Rollinger, J. M.; Hornick, A.; Langer, T.; Stuppner, H.; Prast, H. Acetylcholinesterase inhibitory activity of scopolin and scopoletin discovered by virtual screening of natural products. *J. Med. Chem.* **2004**, *47*, 6248–6254.
- (29) Bartolucci, C.; Perola, E.; Pilger, C.; Fels, G.; Lamba, D. Three-dimensional structure of a complex of galanthamine (Nivalin) with acetylcholinesterase from *Torpedo californica*: Implications for the design of new anti-alzheimer drugs. *Proteins* **2001**, *42*, 182–191.
- (30) Sugimoto, H.; Tsuchiya, Y.; Sugumi, H.; Higurashi, K.; Karibe, N.; Iimura, Y.; Sasaki, A.; Kawakami, Y.; Nakamura, T. Novel piperidine derivatives. Synthesis and anti-acetylcholinesterase activity of 1-benzyl-4-[2-(N-benzoylamino)ethyl]piperidine derivatives. *J. Med. Chem.* **1990**, *33*, 1880–1887.
- (31) Sugimoto, H.; Tsuchiya, Y.; Sugumi, H.; Higurashi, K.; Karibe, N.; Iimura, Y.; Sasaki, A.; Araki, S.; Yamanishi, Y.; Yamatsu, K. Synthesis and structure-activity relationships of acetylcholinesterase inhibitors: 1-benzyl-4-(2-phthalimidoethyl)piperidine, and related derivatives. *J. Med. Chem.* **1992**, *35*, 4542–4548.
- (32) Vidaluc, J.-L.; Calmel, F.; Bigg, D.; Carilla, E.; Stenger, A.; Chopin, P.; Briley, M. Novel [2-(4-Piperidinyl)ethyl](thio)ureas: synthesis and antiacetylcholinesterase activity. *J. Med. Chem.* **1994**, *37*, 689–695.
- (33) Kuroki, Y.; Kimura, T.; Fujiwara, H.; Anpeiji, S. Pyrimidine compound. Patent (PCT Pat. Application), WO 9407890, 1994.
- (34) Takasugi, H.; Kuno, A.; Ohkubo, M. Oxadiazole derivatives having acetylcholinesterase-inhibitory and muscarinic agonist activity. Patent (PCT Pat. Application), WO 93/13083, 1993.
- (35) Gouet, P.; Courcelle, E.; Stuart, D. I.; Metoz, F. ESPript: multiple sequence alignments in PostScript. *Bioinformatics* **1999**, *15*, 305–308.

CI900491T